On Channels with Composite Rough Surfaces at Terahertz Frequencies

Fawad Sheikh[1], Qammer H. Abbasi[2], Thomas Kaiser[1]
[1]Institut für Digitale Signalverarbeitung, Universität Duisburg-Essen (UDE), Campus Duisburg, NRW, Germany
[2]School of Engineering, University of Glasgow (UoG), Glasgow, UK

***Abstract*—The paper preliminarily examines the influence of diffuse reflection by composite rough surfaces in ultra-broadband terahertz (THz) communication channels across 300 GHz (0.3 THz) to 310 GHz (0.31 THz) frequency spectrum. At terahertz frequencies, diffuse reflection tends to be higher due to the increased surface roughness and this surface roughness causes an additional attenuation even in a specular direction of reflection (by the amount that is scattered into non-specular directions). Two most famous modeling approaches, Rayleigh-Rice (R-R) and Beckmann-Kirchhoff (B-K) theories are employed to account for the surface scattering and compared by demonstrating the multipath channel transfer function (CTF) dynamics for line-of-sight (LoS) and non-line-of-sight (NLoS) conditions in a simple office environment. The R-R vector perturbation approach predicts diffuse reflection from optically smooth surfaces ($\sigma_h/\lambda \ll 1$), whilst classical B-K theory in addition attempts to predict the angular distribution of the scattered field from very rough surfaces ($\sigma_h/\lambda \gg 1$). The composite rough surfaces considered in this work have a Gaussian probability density of height and a Gaussian correlation function. Based on these results, it is concluded that the rough surface scattering effects are enhanced at terahertz frequencies and the scattering phenomena show a significant impact, especially in NLoS configuration.**

I. Introduction

Wireless data rates up to 100 Gb/s will be required in 2020 [1]. For example, a forthcoming next generation video format, namely Super Hi-Vision has a resolution of 7680 x 4320, that is sixteen times larger than the current 1080p format, depending on it's frame rate and color depth requires more than 24 Gb/s data rate [2]. In addition, some of the most promising 5G applications such as augmented reality and virtual reality will require in the near future wireless data transmission capacity exceeding several hundred Gb/s. Obviously, these higher quality experiences come at the expense of higher bandwidths. Due to global bandwidth shortage in the microwave region, realization of such high data rates requires undoubtedly a spectral shift to terahertz regime, which offers large swaths of bandwidth (i.e., 20 GHz and beyond) helping pave the way for high speed wireless communications [3].

Terahertz Technology has come of age and the standards of IEEE 802.15.3d-2017 operating from 252 GHz to 325 GHz, designed for data rates of up to 100 Gb/s for intra-device communication (e.g., board-to-board communication), close proximity communication, wireless data centers and backhaul/fronthaul links, are already approved [4].

In order to meet the goals, a spectral window centered at 300 GHz can be utilized that offers 47 GHz of bandwidth [5], which allows a 100 Gb/s high throughput even with a simple modulation scheme. This carrier frequency is the choice of the fortune for two reasons: (i) it is five times higher than the highest frequency of 60 GHz used in wireless communications today; (ii) the atmospheric attenuation is of less extreme falling within the spectral windows. However, to transmit at terahertz frequencies means significant atmospheric attenuation outside spectral windows, notably larger free space path loss, quite high reflection losses, and extreme frequency selective behavior of the propagation mechanism. Moreover, the diffuse reflection from typical interior building materials (e.g., granular wallpaper and plaster walls etc.) becomes more relevant as well as prominent with increasing frequencies, and additionally contributes to multipath propagation due to diffuse components in non-specular directions [6]. Especially, for NLoS schemes where the total received power entirely depends on indirect paths, diffuse reflection phenomena must be regarded in propagation modeling. Indeed, the direct path could be completely blocked by moving objects into the line-of-sight propagation. It should be emphasized that these unique features lead to new models to characterize the multipath THz propagation channel and consequently, need to be addressed by making thorough analysis of ultra-broadband channel behaviour.

In the past, only reckonable ultra-broadband THz channel results based on measurements [7]- [12] have been reported. Nevertheless, the influence of diffuse reflection in the non-specular direction has only been considered by using ray tracing [10]- [12]. In fact, the aforementioned papers focus on short-range wireless links for line-of-sight communication. In our previous work [13] also, we reported the ultra-broadband channel behaviour of both time- and frequency-domain which accounts for reflective properties of rough materials in the specular direction only by ignoring non-specular reflections in the total received power. It is important to notify that none of the former papers have investigated ultra-broadband channel behaviour in a realistic office environment for non-line-of-sight channels. Recently, in experiment [14] first specular NLoS link from a typical indoor wall has been demonstrated at (discrete) terahertz frequencies, opening up a new horizon of scientific investigation for NLoS THz communications.

In this paper, our focus is to illustrate the ultra-broadband channel behaviour by using our self-developed ray tracing algorithm [15] in terms of the frequency-domain channel transfer function dynamics at 3201 frequency points for

f = 300...310 GHz in LoS and NLoS scenarios. The surface scattering process for diffuse reflection has been analyzed using the most prominent analytical scattering theories such as Rayleigh-Rice [16]- [19] and Beckmann-Kirchhoff theory [20]. On the one hand, the diffuse reflection impact from composite rough surfaces in the specular direction has been modeled based on Rayleigh-Rice (R-R) theory (i.e., the specular losses occur due to the diffuse reflection). On the other hand, classical Beckmann-Kirchhoff (B-K) model is implemented accounting for the diffuse reflection in both specular and non-specular directions from composite rough surfaces. To account for the former we use a commercial ray tracer whereas for the latter we employ our ray tracing algorithm (RTA). We call these surfaces in our study as *composite* since the objects in our office environment such as doors, windows, wardrobe, table and plaster walls are composed of multiple materials. The composite materials are optically smooth but not ideally smooth. An ideally smooth surface may be defined as one for which the $\sigma_h = 0$. In [21], it is also shown that most of the ideally smooth materials from lower frequency bands become rough now at THz frequencies and thus scatter.

II. Surface Scattering Models

There are many different analytical methods to solve the surface scattering problem from both optically smooth (or slightly rough) and very rough surfaces. Moreover, these methods can be divided into those which model the effect of roughness on the specular direction of reflection and those that in addition attempt to account for the non-specular diffuse reflection components. Basically, the surface scattering problem is a boundary value problem of Maxwell's equations which is extremely complex but can be simplified by means of approximate models. However, such approximations result in different limitations of their domain of validity. Two most common surface scattering models, Rayleigh-Rice and Beckmann-Kirchhoff, are widely used each having their specific advantages and limitations. For example, R-R approach performs best at arbitrary angles of incidence and scattering but fails for rougher surfaces, whilst B-K approach yields better results for rougher surfaces but fails at wide scattering angles and large angles of incidence due to energy absorption, self shadowing and multiple scattering effects. Furthermore, the B-K model provides closed-form solutions only for slightly rough and very rough surfaces. Whilst the analytical approaches from above make use of the statistical properties of stochastic surfaces instead of relying on the knowledge of the exact topography, this has the advantage of inherent ensemble averaging.

Note that the scattering problems can be classified by the type of rough surface. Depending on the magnitude of the roughness parameter of a material g, which is a straightforward norm of estimating the degree of EM roughness of a surface, i.e., if a surface can be qualified as perfectly smooth ($g = 0$), slightly rough ($0 < g \ll 1$), or very rough ($g \gg 1$) as depicted with its reflection and scattering pattern in Fig. 1.

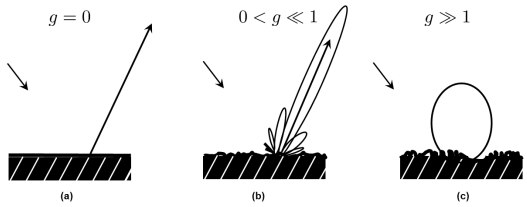

Fig. 1: Schematic diagrams showing specular and diffuse reflection. The surfaces are: (a) perfectly smooth, (b) slightly rough, and (c) very rough.

A. Rayleigh-Rice (R-R) theory

The R-R approach can be seen as the most rigorous analytical solution of Maxwell's equations for the limiting case of optically smooth surface (i.e., slightly rough surface). Rayleigh expressed optical smoothness by following the accurate criterion from [19] as

$$(4\pi\sigma_h \cos\Theta_i/\lambda)^2 \ll 1 \tag{1}$$

Notice that (1) does not contain the scattering angle as an argument. The reason is straightforward, no assumptions were made regarding this angle when developing the theory. Besides, the optically smooth surface check can be a formidable figure depending on the composite surface or wavelength at hand. It is usually formulated as: $\sigma_h/\lambda \ll 1$. Unfortunately, there is no explicit number to decide whether the criterion is fulfilled or not. For example, in [19] and [22] it is stated that σ_h/λ should be smaller than 0.01 and 0.05, respectively. However, in case of THz frequencies, the optically smooth surface requirement is possibly to be reinstated owing to the extremely shorter wavelength. Therefore, in our simulation model, we assume slightly rough surfaces σ_h = 0.15 mm and σ_h = 0.30 mm. We consider σ_h = 0 mm as a benchmark for conceptualization of ideally smooth surfaces as opposed to rough surfaces.

R-R theory was developed on the basis of the boundary conditions for a perfectly conducting surface. Besides, this theory takes polarization of the incident and scattered wave into account. A small parameter of this theory is the Rayleigh roughness parameter (ρ_{spec}). For a Gaussian height probability density function, this term is equal to

$$\rho_{\text{spec}} = e^{-\frac{g}{2}} = \exp\left(-\frac{8\pi^2 f^2 \sigma_h^2 \cos^2\Theta_i}{c^2}\right) \tag{2}$$

where,

$$g = \sigma_h^2(2\pi f/c)^2(\cos(\Theta_i))^2$$

Here, f the frequency of the incident wave, σ_h the standard deviation of the surface roughness, Θ_i the angle of incidence and reflection relative to the surface normal, and c the velocity of light. The expressions for conventional Fresnel reflection coefficient in case of parallel (Γ_{TM}) and perpendicular (Γ_{TE}) polarizations for smooth surfaces are given in [20, p. 21]. Next, the modified reflection coefficient ($\widetilde{\Gamma}$) accounting for

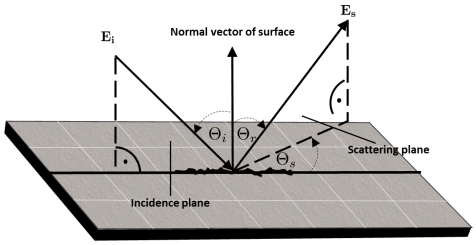

Fig. 2: Illustration of the basic scattering geometry.

the roughness of materials in the THz range are then

$$\widetilde{\Gamma} = \rho_{\text{spec}}\, \Gamma \tag{3}$$

B. Beckmann-Kirchhoff (B-K) theory

The Beckmann-Kirchhoff theory is more realistic and provides more insight of the physical processes involved in the surface scattering. The B-K model is validated against ultra-broadband measurements [10] and it is applicable to both dielectric and metallic surfaces. However, the B-K theory is a scalar treatment; i.e., the wave scattering theory accounts only for the distribution of energy, and does not account for more complex effects such as polarization. The B-K theory is derived from the Helmholz integral [23] and it predicts a symmetrical scattered field distribution about the specular direction under some assumptions for slightly and very rough surfaces [20]. The details of the theory along with its derivation are described comprehensively in the monograph by Beckmann and Spizzichino [20] and we shall only mention the key steps involved in the derivation of the model.

Hereupon, the derived expected value of the square of magnitude of the scattering coefficient ρ of a composite rough surface under the assumptions for infinite conducting surface is

$$\langle \rho\rho^* \rangle_\infty = \left(\rho_0^2 + \frac{\pi \ell_{cr}^2 F^2}{A} \sum_{m=1}^{\infty} \frac{g^m}{m!m} e^{-\frac{v_{xy}^2 \ell_{cr}^2}{4m}} \right) e^{-g} \tag{4}$$

Here, ρ_0 the scattering coefficient of a plane surface of area $\mathrm{A} = l_x l_y$ is given by

$$\rho_0 = \mathrm{sinc}(v_x l_x)\, \mathrm{sinc}(v_y l_y) \tag{5}$$

From trigonometry it follows,

$$v_x = k(\sin(\Theta_i) - \sin(\Theta_r)\cos(\Theta_s)) \tag{6}$$

$$v_y = k(-\sin(\Theta_r)\sin(\Theta_s)) \tag{7}$$

$$v_{xy} = \sqrt{v_x^2 + v_y^2} \tag{8}$$

The geometrical factor, a function of incident and scattered angles is,

$$F = \frac{1 + \cos(\Theta_i)\cos(\Theta_r) - \sin(\Theta_i)\sin(\Theta_r)\cos(\Theta_s)}{\cos(\Theta_i)(\cos(\Theta_i) + \cos(\Theta_r))} \tag{9}$$

The quantity g, a measure of phase variation introduced by surface roughness σ_h is,

$$g = \sigma_h^2 (2\pi f/c)^2 (\cos(\Theta_i) + (\cos(\Theta_r))^2$$

TABLE I: Most significant parameters for surface scattering models

Parameters	Values
Ray tracing method*	SBR
Frequency f	300...310 GHz
Bandwidth B	10 GHz
Simulation points N_f	3201
Office area	7 m (x) x 7 m (y) x 3 m (z)
Antenna type	Omnidirectional
Polarization*	Vertical
TX height (position)	2 m (x = 6, y = 1, z = 2)
RX-LoS height (position)	0.75 m (x = 3.5, y = 4.45, z = 0.75)
RX-NLoS height (position)	0.75 m (x = 1.7, y = 2.75, z = 0.75)
No. of reflections	2
Path loss threshold*	-160 dB
Ray spacing*	0.2°
Waveform	Sinusoid
Transmit power	0 dBm
Tile size**	10 x ℓ_{cr}
No. of tiles*	20x20

* parameter for R-R model
**parameter for B-K model

Owing to (5), B-K model uses two statistical parameters to characterize rough surfaces: (i) the standard deviation height σ_h; (ii) the correlation length ℓ_{cr}. In general, the height values of the topographic surface features about the mean surface level are measured at equally spaced digitized data points. On the other hand, the correlation length ℓ_{cr} is defined as the lag-length at which the Gaussian correlation function drops to $1/e$ of its maximum [23].

The exponential series given by the summation in the lobe component can be approximated for slightly rough ($0 < g \ll 1$) and very rough surfaces ($g \gg 1$). The approximation results in simpler expressions of the scattering coefficient for these two extreme surface conditions are

$$\langle \rho\rho^* \rangle_{\text{slightly rough}} = \left(\rho_0^2 + \frac{\pi \ell_{cr}^2 F^2 g}{A} e^{-\frac{v_{xy}^2 \ell_{cr}^2}{4}} \right) e^{-g} \tag{10}$$

$$\langle \rho\rho^* \rangle_{\text{very rough}} = \frac{\pi \ell_{cr}^2 F^2}{A v_z^2 \sigma_h^2} e^{-\frac{v_{xy}^2 \ell_{cr}^2}{4 v_z^2 \sigma_h^2}} \tag{11}$$

Finally, for finite conducting surfaces, the average scattering coefficient becomes

$$\langle \rho\rho^* \rangle_{\text{finite}} = \langle \Gamma\Gamma^* \rangle \langle \rho\rho^* \rangle_\infty \tag{12}$$

III. Channel Simulations

A. The Indoor THz Channel

The modeling of diffuse reflection by rough surfaces in indoor THz channels is inevitable due to the increasing trend of using formidable range of raw materials (e.g., cinder block, limestone slab, cork sheet etc.) for designing the interior

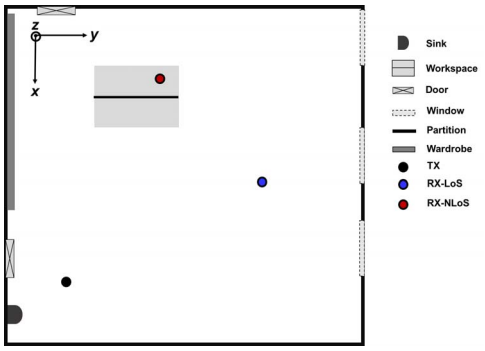

Fig. 3: 2D layout of the BB121 office (top view) showing LoS and NLoS scenario.

of the indoor environments. The dimensions of the height standard deviation (σ_h) of such materials are comparable to or even larger than the wavelength of the incident wave (e.g., $\lambda_{300\text{GHz}} = 1$ mm) and impair the quality of the THz links. The scattering coefficient measurements of such materials have been performed at 300 GHz and results depict the specular lobe constituting additionally a multitude of dominant side lobes in non-specular direction (cf. Fig. 6a-d in [6]). It is an apparent paradox to R-R theory, i.e., (1) does not contain the scattering angle as a factor. The essential terahertz propagation mechanism has been described in detail in our previous work [15], hence, we omit the description here to keep the paper brief.

B. Scenarios and Ray Tracing

The simulation setup is depicted in Fig. 3 and the most significant simulation parameters for both scattering models are combined and given in Table I. For the sake of conciseness, we refer the reader to author's separate publication [24] for the detailed description of the scenario, the ray tracing algorithm and material parameters rather than adding the lengthy description once again in this work.

IV. Results and Discussion

In this section, we demonstrate the ultra-broadband channel transfer function dynamics to assess the channel frequency dispersion behaviour based on the scattering models derived in advance. At THz frequencies, the multipath propagation characteristics are likely to vary significantly over the band of interest in case the environment is surrounded by composite rough surfaces. This is actually the case in our simulation model where all walls and the ceiling are made of composite rough plasters. Furthermore, we alter for rough plaster walls and ceiling the $\sigma_h = 0$ mm, $\sigma_h = 0.15$ mm, and $\sigma_h = 0.30$ mm with focus to demonstrate the influence of degree of roughness on the ultra-broadband terahertz channel. Thus, in order to compare both models, we illustrate in Fig. 4 and 5 the simulation results for LoS and NLoS scenarios, respectively.

Fig. 4 depicts the LoS results with and without scattering. In Fig. 4a and 4b, we can observe in case of no scattering (or no roughness) the highest frequency selectivity of the channel. However, the average attenuation over the whole bandwidth in Fig. 4a is found to be 96.59 dB, 97.02 dB and 100.86 dB for no roughness, R-R and B-K models, respectively. As deduced the average attenuation in case of Fig. 4b for the scattering models is 97.04 dB and 102.4 dB. Intuitively, this almost identical average attenuation for $\sigma_h = 0.15$ mm and $\sigma_h = 0.30$ mm is perhaps highlighting the effect of a dominant line-of-sight path components compared to the scattered channel paths with almost negligible effect. In other words, by varying the σ_h does not affect the relative scattered power in LoS case. The peak-to-peak frequency dependent variations of up to 44 dB at $f = 305.9$ GHz can be clearly seen between no roughness and R-R model in Fig. 4a. For B-K model, this is comparatively lower which is 22 dB. Besides, the calculated standard deviations over the whole bandwidth between smooth environment, R-R, and B-K in Fig. 4a are 5.16 dB, 1.70 dB and 5.96 dB, respectively. Meanwhile, this proves the necessity to include scattering in THz propagation modeling. More or less in Fig. 4b, the average attenuation and the standard deviation gap is somewhat widened since more specular power is scattered out of the specular direction and hence leads to a higher attenuation of the specularly reflected path components. Contrarily, when we compare the R-R or B-K model for $\sigma_h = 0.15$ mm and $\sigma_h = 0.30$ mm, then the channel has hardened. Thus, the channel roughness on one hand increases the scattering richness but on the other hand decreases the channel strength.

Next, NLoS case depicted in Fig. 5 represents very interesting results. In case of R-R, the average attenuation over the band of interest has increased from 110.09 dB to 111.87 dB for increased $\sigma_h = 0.15$ mm to $\sigma_h = 0.30$ mm. Conversely, for B-K model it has reduced from 109.9 dB to 107.97 dB by increasing σ_h. The R-R model demonstrates an inverted behaviour with respect to B-K model. It is important to point out that the R-R model uses only one statistical parameter for the composite rough surface and that is the σ_h. However, the B-K model additionally comprises the correlation length ℓ_{cr}. This gives us the impression that the more the statistical parameters, the better the interpretation of rough surfaces.

V. Conclusion

We have investigated the Rayleigh-Rice and Beckmann-Kirchhoff models at THz frequencies. The R-R model underestimates the impact of scattering from composite rough surfaces on ultra-broadband indoor channels, especially for NLoS case. For LoS case, both models perform well and exhibit little dependence on the surface roughness σ_h. In addition, the comparison between the simulated CTF for smooth environment and scattering models calls for the need to include scattering in THz propagation modeling.

Acknowledgment

The research work presented in this paper has been funded by the German Research Foundation (Deutsche Forschungs-

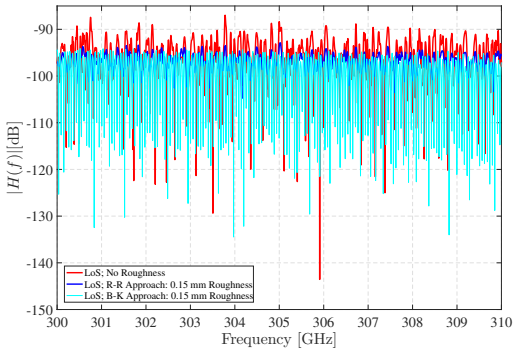

(a) RX-LoS: 0.15 mm Roughness

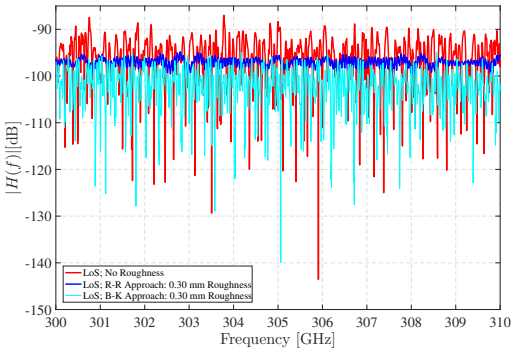

(b) RX-LoS: 0.30 mm Roughness

Fig. 4: Comparison of channel transfer functions between R-R and B-K model at RX-LoS (x = 3.5 , y = 4.45 , z = 0.75).

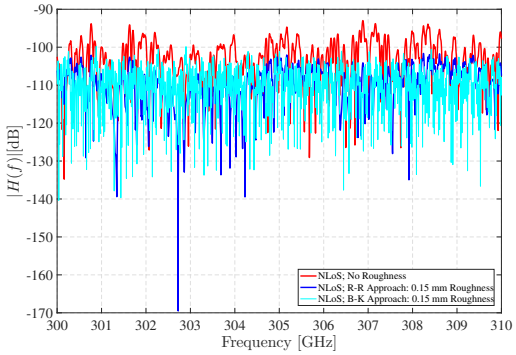

(a) RX-NLoS: 0.15 mm Roughness

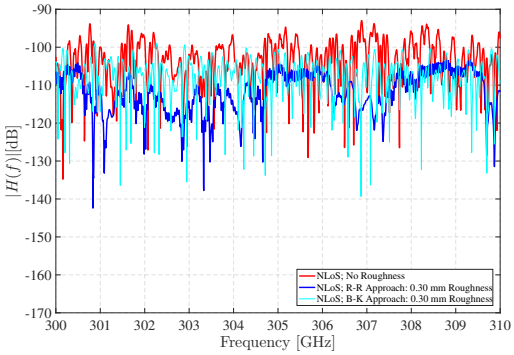

(b) RX-NLoS: 0.30 mm Roughness

Fig. 5: Comparison of channel transfer functions between R-R and B-K model at RX-NLoS (x = 1.7 , y = 2.75 , z = 0.75).

gemeinschaft) under the framework of SFB TRR-196 for the Project M01.

References

[1] S. Cherry, "Edholmes law of bandwidth," *IEEE Spectr.*, vol. 41, no. 7, pp. 58–60, 2004.

[2] H. J. Song and T. Nagatsuma, "Handbook of Terahertz Technologies: Devices and Applications," *Pan Standford Pub*, Singapore, 2015.

[3] F. Sheikh, N. Zarifeh, and T. Kaiser, "Terahertz band: Channel modelling for short-range wireless communications in the spectral windows," in *IET Microwaves, Antennas & Propagation*, vol. 10, no. 13, pp. 1435–1444, 2016.

[4] https://ieeexplore.ieee.org/iel7/8066474/8066475/08066476.pdf, 2017.

[5] M. F. Hermelo, R. Chuenchom, V. Rymanov, T. Kaiser, F. Sheikh, A. Czylwik, and A. Stöhr, "Photonic-Assisted mm-Wave and THz Wireless Transmission towards 100 Gbit/s Data Rate," *Frequenz: Journal of RF-Engineering and Telecommunications*, vol. 71, no. 9-10, pp. 485–498, 2017.

[6] C. Jansen et al., "Diffuse Scattering From Rough Surfaces in THz Communication Channels," in *IEEE Transactions on Terahertz Science and Technology*, vol. 1, no. 2, pp. 462–472, 2011.

[7] S. Priebe et al., "Channel and Propagation Measurements at 300 GHz," in *IEEE Transactions on Antennas and Propagation*, vol. 59, no. 5, pp. 1688–1698, 2011.

[8] S. Priebe et al., "A Measurement System for Propagation Measurements at 300 GHz," *PIERS Proceedings*, pp. 1176–1181, 2010.

[9] S. Kim and A. Zajic, "Statistical Characterization of 300-GHz Propagation on a Desktop," *IEEE Transactions on Vehicular Technology*, vol. 64, no. 8, pp. 3330–3338, 2015.

[10] S. Priebe et al., "Non-specular scattering modeling for THz propagation simulations," *Proceedings of the 5th EUCAP*, pp. 1–5, 2011.

[11] S. Priebe et al., "Polarization Investigation of Rough Surface Scattering for THz Propagation Modeling," *Proceedings of the 5th EUCAP*, pp. 24–28, 2011.

[12] S. Priebe et al., "A comparison of indoor channel measurements and ray tracing simulations at 300 GHz," *35th International Conference on Infrared Millimeter and Terahertz Waves*, pp. 1–2, 2010.

[13] F. Sheikh and T. Kaiser, "Rough Surface Analysis for Short-Range Ultra-Broadband THz Communications," *in IEEE Int. Symposium on Antennas and Propagation*, pp. 1782–1783, 2018.

[14] J. Ma et al., "Channel performance for indoor and outdoor terahertz wireless links," *APL Photonics*, vol. 3, no. 5, pp. 1–12, 2018.

[15] F. Sheikh, D. Lessy, and T. Kaiser, "A Novel Ray-Tracing Algorithm for Non-specular Diffuse Scattered Rays at Terahertz Frequencies," *in 2018 1st IWMTS*, pp. 1–6, 2018.

[16] S. O. Rice, "Reflection of electromagnetic waves from slightly rough surfaces," *Commun. Pure Appl. Math.*, vol. 4, no. 2-3, pp. 351–378, 1951.

[17] E. Church, H. Jenkinson, and J. Zavada, "Relationship between surface scattering and microtopographic features," *Opt. Eng.*, vol. 18, pp. 125–136, 1979.

[18] J. Elson and J. Bennett, "Vector scattering theory," *Opt. Eng.*, vol. 18, pp. 116–124, 1979.

[19] J. Stover, "Optical Scattering, Measurement and Analysis," *2nd. Ed.*, SPIE Press, 1995.

[20] P. Beckmann and A. Spizzichino, "The Scattering of Electromagnetic Waves from Rough Surfaces," *Artech House Radar Library*, USA, 1963.

[21] R. Piesiewicz et al., "Properties of Building and Plastic Materials in the THz Range," *International Journal of Infrared and Millimeter Waves*, vol. 28, no. 5, pp. 363–371, 2007.

[22] T. Vorburger, E. Marx, and T. Lettieri, "Regimes of surface roughness measurable with light scattering," *Appl. Opt.*, vol. 32, no. 19, pp. 3401–3408, 1993.

[23] S. Nayar, K. Ikeuchi, and T. Kanade, "Surface reflection: physical and geometrical perspectives," *IEEE Transactions on Pattern Analysis and Machine Intelligence*, vol. 13, no. 7, pp. 611–634, 1991.

[24] F. Sheikh, D. Lessy, M. Alissa, and T. Kaiser, "A Comparison Study of Non-specular Diffuse Scattering Models at Terahertz Frequencies," *in 2018 1st IWMTS*, pp. 1–6, 2018.